Z. Phys. B 91, 113–125 (1993)

Condensed
Zeitschrift für Physik B Matter

Finite size effects at thermally-driven first order phase transitions: a phenomenological theory of the order parameter distribution

Katharina Vollmayr, Joseph D. Reger, Manfred Scheucher, Kurt Binder

Institut für Physik, Johannes Gutenberg Universität Mainz, Staudinger Weg 7, W-6500 Mainz, Germany

Received: 11 November 1992

Abstract. We consider the rounding and shifting of a first-order transition in a finite d-dimensional hypercubic L^d geometry, L being the linear dimension of the system, and surface effects are avoided by periodic boundary conditions. We assume that upon lowering the temperature the system discontinuously goes to one of q ordered states, such as it e.g. happens for the Potts model in $d=3$ for $q \geqq 3$, with the correlation length ξ of order parameter fluctuation staying finite at the transition. We then describe each of these q ordered phases and the disordered phase for $L \gg \xi$ by a properly weighted Gaussian. From this phenomenological ansatz for the total distribution of the order parameter, all moments of interest are calculated straight-forwardly. In particular, it is shown that for L exceeding a characteristic minimum size $L_{\min}$ the forth-order cumulant $g_L(T)$ exhibits a minimum at $T_{\min} > T_c$, with $T_{\min} - T_c \propto L^{-d}$ and the value of the cumulant at the minimum ($g(T_{\min})$) behaving as $g(T_{\min}) \propto L^{-d}$. All cumulants $g_L(T)$ for $L \gg \xi$ approximately intersect at a common crossing point $T_{\text{cross}} \propto L^{-2d}$, with a universal value $g(T_{cross}) = 1 - n/2q$, where n is the order parameter dimensionality. By searching for such a behavior in numerical simulation data, the first order character of a phase transition can be asserted. The usefulness of this approach is shown using data for the $q=3$, $d=3$ Potts ferromagnet.

1. Introduction

Phase transitions involve a singular behavior of the free energy of a many body system, and are possible in the thermodynamic limit (volume $V \to \infty$) only, while in finite systems no such singularities are possible; i.e., for V finite, a transition that is sharp and well defined for $V \to \infty$, is somewhat diffuse and rounded, and relative to the critical parameter value where it occurs for $V \to \infty$ also a shift of the transition region may occur. Such finite size effects on phase transitions are not only of interest from the point of view of the foundations of statistical mechanics and for the interpretation of pertinent experiments, but are crucial for the interpretation of Monte Carlo and Molecular Dynamics computer simulations [1–6], which always deal with finite systems. A theoretical understanding of such finite size effects is a prerequisite for estimating precisely the value of a control parameter (temperature, pressure, non-ordering fields [7, 8], etc.) for which a transition occurs; also distinguishing whether a transition is second order [7] or first order [8] sometimes is a challenge. Finally, characterizing the finite size effects is necessary for estimating quantitatively properties of interest at a transition from simulations (for a second order transition, one is interested in critical exponents and critical amplitudes, for a first-order transition, one is interested in the magnitudes of the discontinuities of various first derivatives of the free energy at the transition such as order parameter, internal energy [and thus the knowledge of the latent heat], etc.).

In this situation, it is no surprise at all that finite size effects at phase transitions have received a long-standing and intensive interest ([9–15] contain review articles and books on this subject, the original literature being far too extensive to be listed here). On the contrary, it is rather surprising that hitherto finite size effects on the order parameter and its various moments, which are extensively discussed for second-order transitions [11–17], at first-order transitions have hardly received any attention. In fact, finite size effects on first-order transitions have found attention only rather recently [18–38]; the order parameter was considered for transitions driven by the field conjugate to the order parameter [21–24], while the work on thermally driven first-order transitions focused on the behavior of the energy distribution and its moments [25–36], although observations on the finite size rounded order parameters are occasionally reported [37, 38].

The present work (preliminary results have been also reported in [39]) tries to fill in this gap, presenting a phenomenological discussion of the order parameter distribution at first-order transitions for finite systems sat-

isfying the condition $L \gg \xi$; because if the linear dimension by far exceeds the correlation length of order parameter fluctuations, for each pure phase the distribution function can be described by a simple gaussian [40]. By a treatment similar to field-driven first-order transitions [22] and to the energy distribution at temperature-driven first-order transitions [25–27], one can describe the finite size effects on the total order parameter distribution and on resulting moments rather satisfactorily. The resulting predictions compare favorable with numerical results for the three-dimensional $q=3$ state Potts model [41, 42].

The outline of the remainder of this paper is as follows. Section 2 develops the general theory, while Sect. 3 gives details on the case of one-component order parameters (this is of interest for cases where a first-order transition to an ordering of Ising type occurs, which happens in Ising systems exhibiting tricritical points [43], certain models for structural phase transitions [44], etc.). Section 4 discusses the case of n-component order parameters, paying particular attention to $n=2$ (the q-state Potts model [41, 42] with $q=3$ belongs to this class). Finally, Section 5 contains a discussion and compares the phenomenological predictions to numerical results from Monte Carlo simulations [37, 45].

2. The phenomenological theory and its basic assumptions

In this section, the concepts and ideas of our approach will be described in detail in order to show clearly the physical assumptions that need to be made. Unlike [26, 27], we are not aiming at any mathematical rigor, but rather rely on the plausibility and obvious simplicity of that approach.

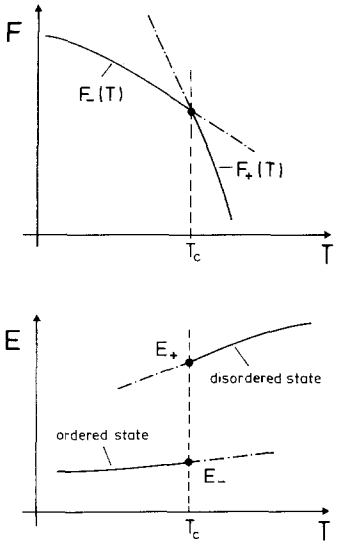

Fig. 1. Schematic plot of the free energy F per lattice site versus temperature T (upper part) and of the internal energy E per lattice site (lower part), for a temperature driven first-order transition T_c. The two branches of the free energy are denoted as $F_-(T)$ {ordered states at low temperatures} and as $F_+(T)$ {disordered states at high temperatures}, respectively. Corresponding energies at T_c are denoted as E_- and E_+, respectively. Dash-dotted parts of the curves represent metastable states, observable at least in a finite box as considered here

The basic idea is that for a first-order transition one has in a finite system a coexistence of the ordered state and the disordered state for some range of temperatures around the transition point (Fig. 1). Such metastable states, although their precise meaning in the thermodynamic limit is certainly subtle [8], are ubiquitously observed in actual simulations. The probability of observing a metastable state is controlled by the free energy difference $\Delta F \equiv F_+ - F_-$. We first introduce relative weights a_+, a_- (which will be normalized later) of the respective different states,

$$a_+ = \exp\{-\Delta F L^d/(2k_B T)\},$$
$$a_- = \exp\{+\Delta F L^d/(2k_B T)\}. \tag{1}$$

In the normalization, one has to consider that for the q-state Potts model there are q distinct ordered states but there is a single disordered phase, of course.

Expanding now the free energy difference in Fig. 1 linearly in $\Delta T \equiv T - T_c$,

$$F_\pm = E_\pm - TS_\pm, \quad \Delta F(T_c) = 0,$$
$$\Rightarrow \Delta F \approx -(E_+ - E_-)\,\Delta T/T_c, \tag{2}$$

the weights a_+, a_- are expressed in terms of the latent heat $E_+ - E_-$ and the volume $V = L^d$ as

$$a_+ \approx \exp\left\{+\frac{(E_+ - E_-)\,\Delta T}{2k_B T_c^2} L^d\right\},$$
$$a_- \approx \exp\left\{-\frac{(E_+ - E_-)\,\Delta T}{2k_B T_c^2} L^d\right\}. \tag{3}$$

By the sign $\approx$ in (2, 3) we wish to emphasize that ΔF is only correct to leading order in ΔT, but this will suffice for large L.

For a discussion of the order parameter distribution, it is of course necessary to consider the order parameter dimensionality n (number of order parameter components) and the symmetry of the Hamiltonian in the space spanned by these components [37, 46, 47]. For simplicity, we mostly consider Potts models [41, 42], but the generalization to other systems is fairly obvious.

The q-state Potts Hamiltonian is

$$\mathcal{H} = -\sum_{\langle i,j \rangle} J_{ij}\,\delta_{S_i S_j} \quad \text{with } S_i \in \{1, 2, \ldots, q\}. \tag{4}$$

While there is a degeneracy between the q different ordered states, the order parameter dimensionality only is $n = q-1$. For example $q=2$ is the usual Ising model which has $n=1$. A simple way to see this in general is to transform to the "simplex representation": one introduces a q-dimensional space formed by q orthogonal unit vectors $\mathbf{S}_i \in \{\hat{e}_1, \ldots, \hat{e}_q\}$, i.e. $\mathcal{H} = -\sum_{\langle i,j \rangle} J_{ij}\,\mathbf{S}_i \cdot \mathbf{S}_j$. Then the q unit vectors in the q-dimensional space are projected on the $(q-1)$ dimensional hyper-tetrahedron (which simply is a triangle for $q=3$, see Fig. 2). This

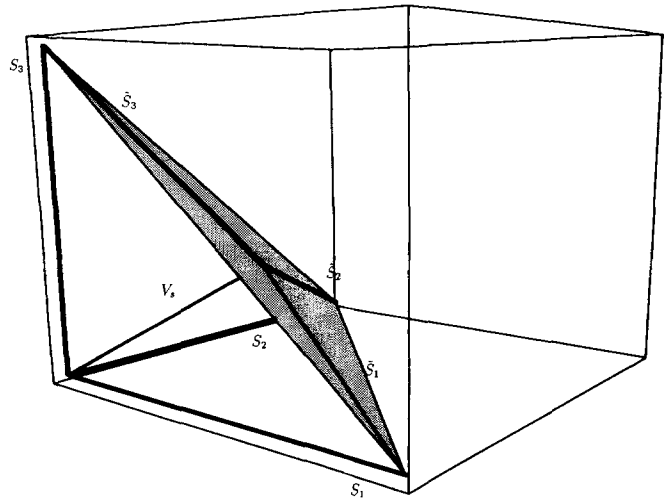

Fig. 2. Introduction of the simplex representation for the 3-state Potts model. The three states $p=1, 2, 3$ are represented by three orthogonal unit vectors $\mathbf{S}_1, \mathbf{S}_2, \mathbf{S}_3$. Connecting their ends one forms the shaded triangle. Connecting then in this plane the ends with the center of gravity (i.e., subtracting from $\mathbf{S}_i$ the vector $\mathbf{V}_s$ to the center of gravity) one forms three vectors $\tilde{\mathbf{S}}_i$ in the shaded plane

yields a Hamiltonian

$$\mathscr{H} = -\sum_{\langle i,j\rangle} \tilde{J}_{ij}\,\tilde{\mathbf{S}}_i\cdot\tilde{\mathbf{S}}_j, \qquad J_{ij}=q\tilde{J}_{ij}/(q-1),$$

$$\tilde{\mathbf{S}}_i\in(\tilde{\mathbf{S}}_1, \tilde{\mathbf{S}}_2, \ldots, \tilde{\mathbf{S}}_q). \tag{5}$$

We now define order parameter components m_μ as follows, N being the number of lattice sites,

$$m_\mu=(1/N)\sum_{i=1}^{N}\tilde{S}_i^\mu, \qquad \mu=1, 2, \ldots, q-1, \tag{6}$$

where the $\tilde{S}_i^\mu$ are the components of the projected and normalized vectors $\tilde{\mathbf{S}}_i$ according to an orthonormalized basis in the $(q-1)$ dimensional space with $\hat{\mathbf{e}}_1=\tilde{\mathbf{S}}_1$. Mostly one is interested in rotationally invariant quantities in the order parameter space, such as the absolute value of the order parameter

$$m=\left(\sum_{\mu=1}^{q-1} m_\mu^2\right)^{1/2}. \tag{7}$$

Hence we shall construct the associated distribution $P_L(m)$ from the distribution of the components $P_L(m_1, m_2, \ldots, m_{q-1})$.

In the disordered phase (+), the distribution

$$P_L(m_1, m_2, \ldots, m_{q-1})$$

is expected to have a Gaussian peak in all $n=p-1$ variables centered at $m_\mu=0$,

$$P_L^+(m_1, m_2, \ldots, m_n)\,dm_1, \ldots, dm_n = h\left(\frac{L^d}{2\pi k_B T\chi_+}\right)^{n/2}$$

$$\cdot\exp\left\{-\frac{m^2L^d}{2k_BT\chi_+}\right\}dm_1, \ldots, dm_n, \tag{8}$$

where h is the normalized relative weight of the disordered phase, which is proportional to $a_+\{(3)\}$. The "susceptibility" χ_+ characterizes the order parameter fluctuations in the disordered phase. Again we emphasize that (8) makes sense only for $L\gg\xi_+$, the correlation length of order parameter fluctuations as T reaches T_c from above. But this limit is always reached for a first-order transition with a discrete number of ordered states, when $L\to\infty$, since then ξ_+, ξ_- remain finite at T_c.

Transforming the multivariate Gaussian to the distribution $P_L^+(m)$ of the absolute value, one gets a phase space factor, $m^{n-1}\Omega_n$, where Ω_n is the surface area of a n-dimensional unit sphere:

$$P_L^+(m)\,dm = h\frac{\Omega_n m^{n-1}L^{nd/2}}{(2\pi k_B T\chi_+)^{n/2}}\exp\left\{-\frac{m^2L^d}{2k_BT\chi_+}\right\}dm. \tag{9}$$

The peak of this distribution is no longer at $m=0$, unlike the multivariate Gaussian, (8), but rather at $m_{\max}=\sqrt{n-1}(k_BT\chi_+/L^d)^{1/2}$.

Now in a model with a q-fold degenerate ordered phase such as the q-state Potts ferromagnet one expects

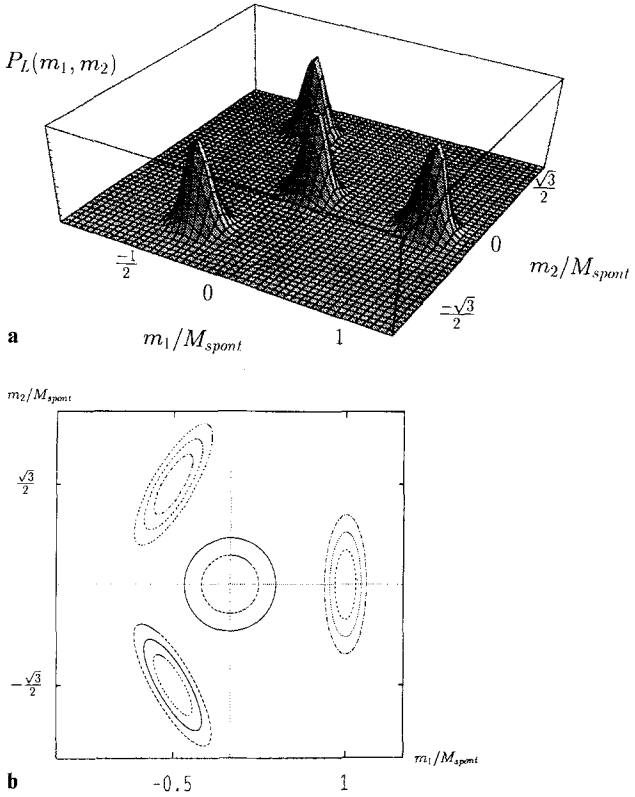

Fig. 3. a Schematic picture of the order parameter distribution $P(m_1, m_2)$ of the three-state Potts model at T_c, where one assumes that the peak of the disordered phase (in the center of the figure) has equal weight (i.e., "volume" underneath the shaded surface) as each of the ordered peaks. Note that m_1, m_2 are plotted in units of the spontaneous order parameter M_{spont} at the transition. **b** Schematic contour plot of the distribution $P_L(m_1, m_2)$ of the order parameter for the $q=3$ state Potts ferromagnet. Order parameter components m_2 (along the ordinate) and m_1 (along the abscissa) are plotted in units of the spontaneous "magnetization" M_{spont} as in **a**. Curves indicate lines of $P_L(m_1, m_2)=\text{const}$

q peaks representing the possible ordered phases (Fig. 3a). For $q=3$, these peaks are expected at positions (using the spontaneous magnetization M_{spont} as unit for the order parameter)

$$(1,0), \quad \left(-\frac{1}{2}, \frac{\sqrt{3}}{2}\right) \quad \text{and} \quad \left(-\frac{1}{2}, -\frac{\sqrt{3}}{2}\right)$$

in the (m_1, m_2)-plane, see Fig. 3b. Of course, one should not expect that one simply has to shift the origin of the above multivariable Gaussian to the respective positions in the (m_1, m_2)-plane, since directions "longitudinal" and "transverse" in order parameter space are no longer equivalent. This is indicated by the effective shape of the contours of the ordered peaks in the contour diagram (Fig. 3b). This qualitative consideration is in agreement with the explicit Monte Carlo calculation of $P_L(m_1, m_2)$ for the 3-state Potts ferromagnet due to Kikuchi and Okabe [37] and Stephanov and Tsypin [46]. Note that the numerical study of $P_L(m_1, m_2)$ in these papers shows that unlike the qualitative Fig. 3b suggests transverse fluctuations are suppressed in comparison to longitudinal ones. The peak at $(m_1, m_2) = M_{\text{spont}}(1, 0)$ can be written as

$$P_L^{(1)}(m_1, m_2) = \frac{1-h}{3} \frac{L^{d/2}}{(2\pi k_B T \chi_l)^{1/2}} \frac{L^{d/2}}{(2\pi k_B T \chi_t)^{1/2}} \times \exp\left\{-\frac{(m_1 - M_{\text{spont}})^2 L^d}{2 k_B T \chi_l}\right\} \times \exp\left\{-\frac{m_2^2 L^d}{2 k_B T \chi_t}\right\}. \tag{10}$$

The other two peaks $P_L^{(2)}(m_1, m_2)$ and $P_L^{(3)}(m_1, m_2)$ are obtained from $P_L^{(1)}$ by a rotation by 120° or 240° in the (m_1, m_2)-plane, respectively. In (10) it is used explicitly that all three peaks of the ordered phase are equivalent and thus have equal weight $(1-h)/3$. Of course, (10) holds only in the limit $L \gg \xi_-$, the correlation length of the order parameter fluctuations for $T \to T_c$ from below. These correlation lengths also appear as exponential corrections in the size-dependence of the quantities χ_+, χ_l, M_{spont} in the distributions (9), (10),

$$\begin{aligned} \chi_+ &= \chi_+^\infty + \chi_+^c \exp(-L/\xi_+), \\ \chi_l &= \chi_l^\infty + \chi_l^c \exp(-L/\xi_-), \\ M_{\text{spont}} &= M_{\text{spont}}^\infty + M_{\text{spont}}^c \exp(-L/\xi_-), \end{aligned} \tag{11}$$

where χ_+^c, χ_l^c and M_{spont}^c are amplitude factors, while the quantities with the superscript infinity apply in the thermodynamic limit. For simplicity, we shall not be concerned with the distinction between χ_+ and χ_+^∞ (χ_l and χ_l^∞, M_{spont} and M_{spont}^∞) in the following, and disregard also related effects for the energies that enter the weighting factors (2), (3)

$$\{E_\pm = E_\pm^\infty + E_\pm^c \exp(-L/\xi_\pm)\}.$$

The total distribution of the ordered phase becomes

$$P_L^-(m_1, m_2) = P_L^{(1)}(m_1, m_2) + P_L^{(2)}(m_1, m_2) + P_L^{(3)}(m_1, m_2). \tag{12}$$

Equations (10), (12) clearly reflect the anisotropy of the orderings in the (m_1, m_2) space. For an isotropic XY-model [7, 47], on the other hand, we would have a distribution with full rotational symmetry in the (m_1, m_2)-plane, of course.

Also the distribution $P_L^-(m_1, m_2)$ is transformed to the distribution $P_L^-(m)$ for the absolute value of the order parameter in the ordered phase. For large L, this distribution is sharply peaked at $m \approx M_{\text{spont}}$. Since in this limit $m \approx m_1$ in (10), m_2 can be integrated over and hence one is left with a simple Gaussian peak for the ordered phase,

$$P_L^-(m) = (1-h) \frac{L^{d/2}}{(2\pi k_B T \chi_-)^{1/2}} \exp\left\{-\frac{(m - M_{\text{sp}})^2 L^d}{2 k_B T \chi_-}\right\}. \tag{13}$$

Here the effective susceptibility of the ordered phase is denoted as χ_-, for the sake of symmetry of the notation ($\chi_- \approx \chi_l$, as should be obvious from the above arguments). Note that while (10), (12) refer to the case $q=3$ only, (13) should hold for general q. It does not hold, however, for an isotropic XY-model, for instance, where a phase space factor $\Omega_2 m$ would appear {similar to (9)!} in (13) as well.

The total distribution of the absolute value of the order parameter then simply becomes the sum of (9) and (13), see Fig. 4,

$$P_L(m) \approx h m^{n-1} \Omega_n \frac{L^{nd/2}}{(2\pi k_B T \chi_+)^{n/2}} \exp\left\{-\frac{m^2 L^d}{2 k_B T \chi_+}\right\} + (1-h) \frac{L^{d/2}}{(2\pi k_B T \chi_-)^{1/2}} \exp\left\{-\frac{(m - M_{\text{spont}})^2}{2 k_B T \chi_-} L^d\right\}. \tag{14}$$

Here the caveat needs to be made that this approximation is valid only near $m \approx 0$ (the disordered phase) and near $m \approx M_{\text{spont}}$ (the ordered phase), for $L \to \infty$, in between the peaks the actual distribution would be dominated by interfacial contributions [17], which are outside of consideration here. The weight h can be written as

$$h = a_+/(a_+ + q a_-) = 1 \Big/ \left\{1 + q \exp\left[-\frac{E_+ - E_-}{k_B T_c^2} \Delta T L^d\right]\right\}. \tag{15}$$

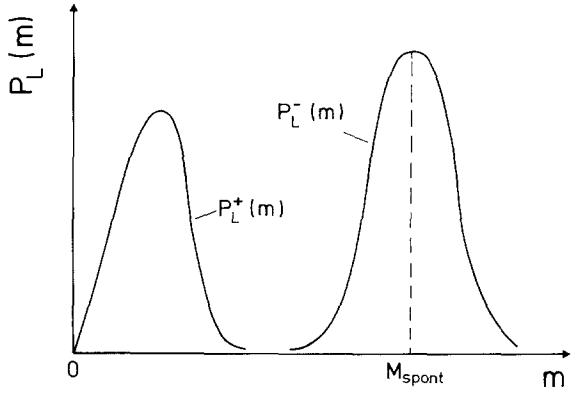

Fig. 4. Schematic plot of the distribution $P_L(m)$ for the absolute value of the order parameter m for $n=2$ near the temperature T_c of the first-order transition

Equations (14), (15) are the central result of our phenomenological theory. We believe it to be valid for general n (including $n=1$, the one-component first-order transition), for anisotropic systems with q distinct phases (isotropic n-component order parameters are not considered here). From (14), (15), it is straightforward (but somewhat tedious) to obtain all moments of interest, k being a positive integer,

$$\langle m^k\rangle_{T,L} \equiv \int_0^1 m^k (P_L(m)\,\mathrm{d}m; \tag{16}$$

of particular interest is the reduced fourth order cumulant $g_L(T)$, which we define here as follows

$$g_L(T) \equiv \left[\frac{\langle m^4\rangle}{\langle m^2\rangle^2}\bigg|_{T\to\infty,L\to\infty} - \frac{\langle m^4\rangle}{\langle m^2\rangle^2}\bigg|_{T,L}\right] \Big/ \left[\frac{\langle m^4\rangle}{\langle m^2\rangle^2}\bigg|_{T\to\infty,L\to\infty} - \frac{\langle m^4\rangle}{\langle m^2\rangle^2}\bigg|_{T=0,L\to\infty}\right]. \tag{17}$$

A detailed discussion of the properties of $P_L(m)$ and the moments $\langle m^k\rangle_{T,L}$ and the cumulant $g_L(T)$ will be deferred to the next sections; here we only note that it is convenient to introduce rescaled variables, such as the rescaled order parameter $\phi = m/M_{\text{spont}}$ and the rescaled linear dimension l, defined by

$$l^d = M_{\text{spont}}^2 L^d/(2k_B T_c \chi_-). \tag{18}$$

This means that the linear dimension L of the lattice is rescaled with a thermodynamic length, as it has appeared to be useful in finite size scaling of critical systems at dimensionalities where the Landau theory of phase transitions holds [11, 13].

The temperature scale is then set by a constant A given by

$$A = (E_- - E_+)\,\chi_-/(M_{\text{spont}}^2 T_c), \tag{19}$$

so h gets simply expressed as

$$h = 1/\{1 + q\exp[2A(T-T_c)\,l^d]\}. \tag{20}$$

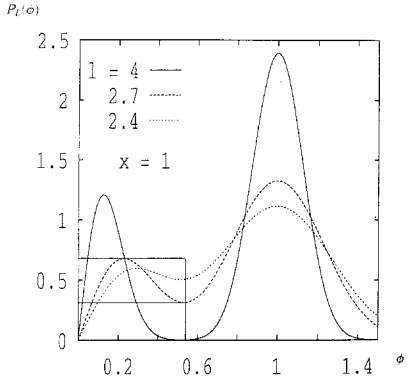

Fig. 5. Plot of distributions $P_l(\phi)$ versus the rescaled order parameter ϕ at $T=T_c$, for $n=2$, $x=1$ and several choices of the rescaled linear dimension l. The distribution has a minimum $P_{\min}=P_l(\phi_{\min})$ at some value $\phi=\phi_{\min}$. The critical linear dimension l_{crit} is defined as $P_{\min}=(1/2)\,P_l(\phi_{\max}^{\text{dis}})$ where $\phi_{\max}^{\text{dis}}$ is the order parameter at the peak value of the disordered phase

The only nontrivial system parameter remains the susceptibility ratio at the transition point. We find it convenient to use the abbreviation

$$x = \sqrt{\chi_+/\chi_-}. \tag{21}$$

Of course, the present multiple Gaussian approximation for $P_L(m_1, \ldots, m_n)$ is applicable only, if at T_c the peaks of $P_L(\phi)$ corresponding to the ordered and disordered phase are still well separated from each other. This im-

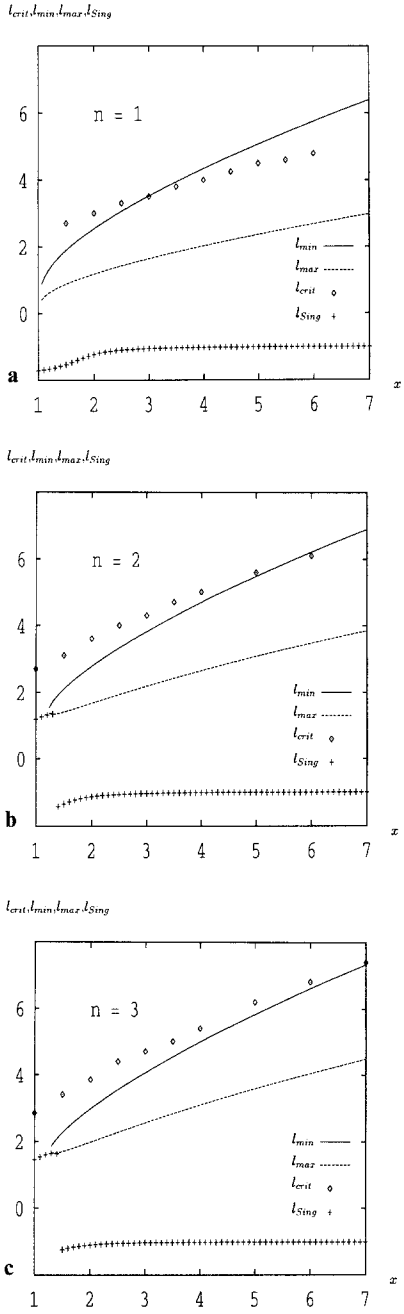

Fig. 6a–c. Characteristic lengths l_{crit}, $l_{\min}$, $l_{\max}$, l_{sing} plotted vs. x for $d=3$ and $n=1$ **a**, $n=2$ **b** and $n=3$ **c**. For a definition of these lengths cf. text. For $n=4$ the behavior is hardly distinguishable from $n=3$ and thus not shown

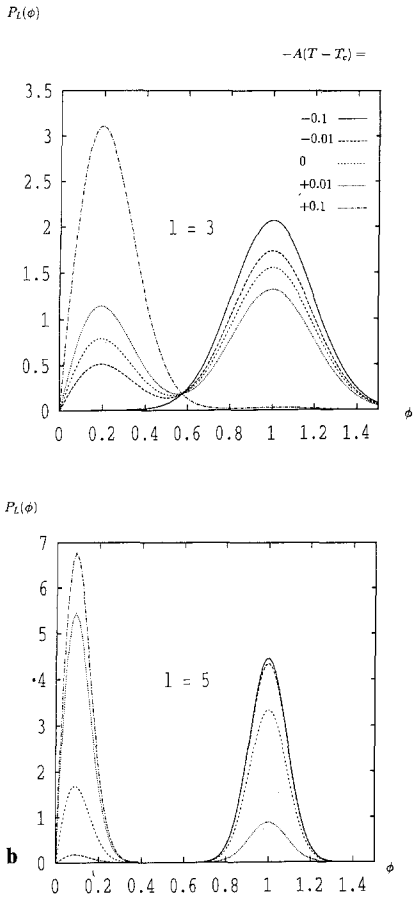

Fig. 7a, b. Plot of $P_l(\phi)$ vs. ϕ for the case $d=3$, $x=1$, $n=2$ and two choices of l: $l=3$ **a** and $l=5$ **b**. Different curves indicate choices of the temperature variable $t=-A(T-T_c)$, as indicated in the figure

plies that l must exceed some minimum value l_{crit}, in order for the present approximations to be applicable. As a minimal choice for l_{crit}, we require that the minimum is at half the height of the peak of the disordered phase. As an example, Fig. 5 illustrates the variation of $P_L(\phi)$ with l at $T=T_c$ in a typical case. It turns out that the precise values of l_{crit} can only be found numerically (Fig. 6). In general, one finds that l_{crit} increases with increasing x. Figure 6 also includes other characteristic linear dimensions $l_{\min}$, $l_{\max}$, l_{sing} that will be discussed in the next section. It also has been checked that at $T=T_c$ there is indeed the strongest overlap between the disordered peak in (14) and the ordered one. Figure 7 shows an example where the temperature is varied. This also suggests two approximations that will be used for the computations of the moments {(16)} throughout: we may extend the integration interval for the disordered part of the distribution for the region of interest ($l \gg l_{\text{crit}}$) from $\phi=0$ to $\phi=\infty$, since for $\phi \gtrsim M_{\text{spont}}^{-1}$ the part of the distribution $P_l^+(\phi)$ corresponding to the disordered phase $\{P_L^+(m)\}$ is negligibly small. Similarly, the integration interval for the part of the distribution $P_l^-(\phi)$ corresponding to the ordered phase $\{P_l^-(m)\}$ can be taken to run from $-\infty$ to $+\infty$, since $P_l^-(\phi)$ is nonzero for $\phi \approx 1 (m \approx M_{\text{sp}})$ only. Thus (16) becomes

$$\langle \phi^k \rangle_{T,l} = \langle m^k \rangle_{T,L} / M_{\text{spont}}^k = \int_0^{M_{\text{spont}}^{-1}} \phi^k P_l(\phi)\, \mathrm{d}\phi$$

$$\approx \int_0^{\infty} \phi^k P_l^+(\phi)\, \mathrm{d}\phi + \int_{-\infty}^{+\infty} \phi^k P_l^-(\phi)\, \mathrm{d}\phi. \tag{22}$$

In this approximation, the reduced moment $\langle \phi^k \rangle_{T,l}$ is no longer dependent on the spontaneous order parameter M_{spont} at the transition. In the example shown in Fig. 7, it is clear that (22) involves a small error for $l=3$, while the error already for $l=5$ is completely negligible. Figure 7 also nicely illustrates the effect of the temperature variable $t=-A(T-T_c)$ which controls the relative weights of the disordered and ordered states, respectively. Note also that rescaled linear dimension l and dimensionality d do not enter the formalism separately, but it is only the rescaled system volume l^d that enters. Of course, this is expected quite generally for first-order transitions in hypercubic geometry with periodic boundary conditions, that it is simply the system volume $V=L^d$ that controls finite size effects [18–27].

The fact that the minimum value l_{crit} where our approximations break down increases with the parameter x is simply understood from the rescaled distribution:

$$P_l(\phi) = h \phi^{n-1} \Omega_n \frac{l^{nd/2}}{(2\pi)^{n/2} x^n} \exp(-\phi^2 l^d / x^2)$$
$$+ (1-h) \frac{l^{d/2}}{(2\pi)^{1/2}} \exp\{-(\phi-1)^2 l^d\}, \tag{23}$$

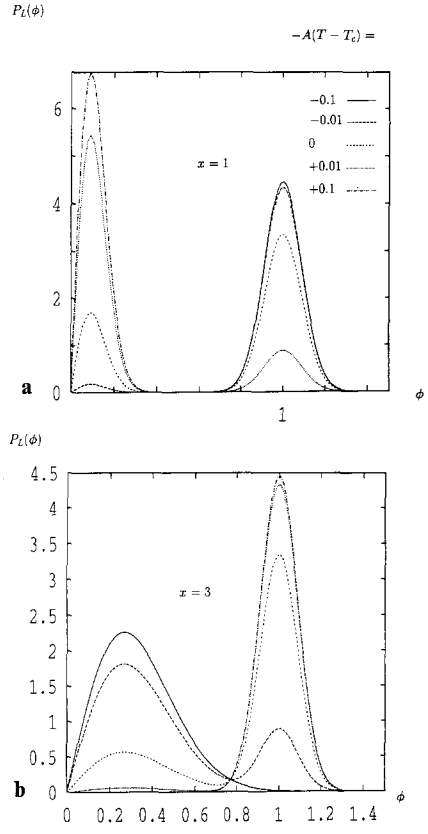

Fig. 8a, b. Plot of $P_l(\phi)$ vs. ϕ for the example $n=2$, $l=5$, $d=3$ and two choices of x: $x=1$ **a** and $x=3$ **b**. Several choices of t are included, as indicated in the figure

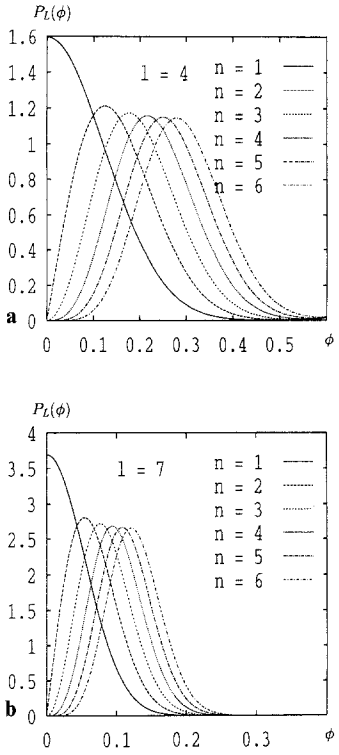

Fig. 9a, b. Plot of $P_l(\phi)$ vs. ϕ for the example $h=1/4$, $x=1$, $d=3$, and two choices of l: $l=4$ **a** and $l=7$ **b** Several choices of n are included, as indicated in the figure

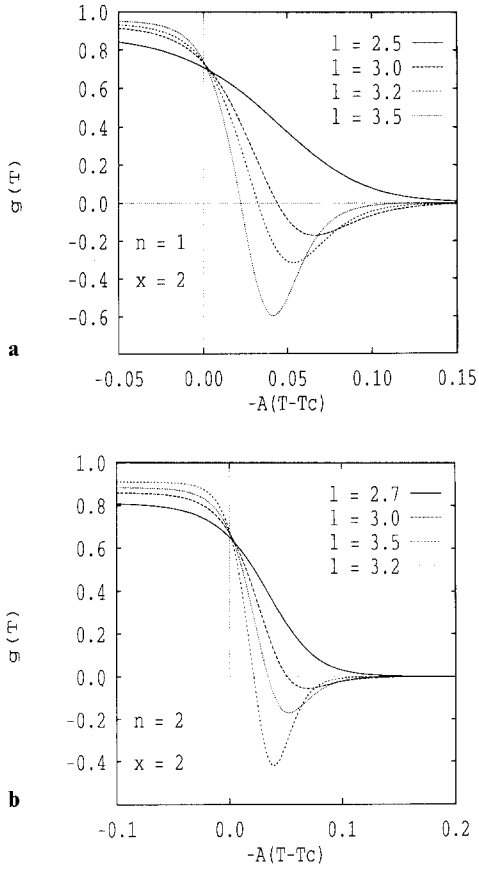

Fig. 10 a, b. Plot of the reduced fourth-order cumulant $g_L(T)$ vs. the temperature variable t for the case $x=2$, $n=1$ **a** and $n=2$ **b** Several choices of l are included, as indicated in the figure

with increasing x the width of the peak corresponding to the disordered phase increases in comparison with the width of the peak corresponding to the ordered phase, and thus their overlap increases and thus also $P_{\min}$ increases (Fig. 8). Finally we discuss the effect of varying the order parameter dimensionality n (Fig. 9). With increasing n the position of the disordered peak moves to larger values of ϕ,

$$\phi_{\max}^{\text{dis}} = \sqrt{n-1}\, l^{-d/2} x \quad \text{while} \quad \phi_{\max}^{\text{ord}} = 1$$

independent of n. Note that the limit $n \to \infty$ in this case is rather subtle, since then also (for a Potts model with $q \to \infty$ distinct phases) the overwhelming configurational entropy implies $T_c \to 0$ [42].

In the last part of this section, we discuss the reduced fourth-order cumulant $g_L(T)$, (17), which can also be written as

$$g_l(T) = \frac{n}{2}\left(1 + \frac{2}{n} - \langle\phi^4\rangle / \langle\phi^2\rangle^2\right). \tag{24}$$

Figure 10 gives typical examples. It is seen that curves for different l seem to have a common intersection point at the transition temperature T_c (or at least very close to it), and in addition $g_L(T)$ develops a minimum at negative values for $T > T_c$; this minimum becomes deeper (and closer to the transition temperature) as l increases. These characteristic features of $g_L(T)$ can in fact be generally derived from (22)–(24), as outlined below (more details can be found in [45]). First we note that $g_L(T)$ depends on T only via the weight h, (20) and hence we find the temperature of the minimum $T_{\min}$ from

$$\left.\frac{dg}{dT}\right|_{T_{\min}} = \left.\frac{dg}{dh}\right|_{h_{\min}} \times \frac{dh}{dT} = 0, \tag{25}$$

where the monotonic variation of h with T implies that the minimum of $\frac{dg}{dh} = 0$ at $h_{\min}$ needs to be sought,

$$h_{\min} = (a_1 b_2 + a_2 b_2 - 2 a_2 b_1)/[(a_2 - a_1)(b_2 - b_1)], \tag{26}$$

where the abbreviations a_1, a_2, b_1, b_2 have the following meaning

$$a_1 = n(n+2)\, x^4 l^{-2d}, \tag{a}$$
$$a_2 = 1 + 6 l^{-d} + 3 l^{-2d}, \tag{b}$$
$$b_1 = n x^2 l^{-d}, \tag{c}$$
$$b_2 = 1 + l^{-d}. \tag{d} \quad (27)$$

From (20) we obtain

$$T_{\min} = T_c + (2A)^{-1} [\ln(h_{\min}^{-1} - 1) - \ln q]\, l^{-d}. \tag{28}$$

It is seen that such a minimum exists only for $h_{\min} < 1$. Hence there exists a minimum value of l, $l_{\min}$, where

$h_{\min}=1$ and such a minimum first appears for $T_{\min}\to+\infty$. As $l>l_{\min}$, this minimum moves towards T_c, as is obvious from (28). This minimum size $l_{\min}$ needed for a non-monotonic temperature variation of $g_l(T)$ is simply found from (26) as the solution of the equation

$$(a_1+a_2)\,b_1=2a_1\,b_2 \tag{29}$$

which requires to find the zeroes of a polymonial of degree 3 in the variable l^{-d}. The first two zeroes can be found at

$$l_{\substack{\min\\ \max}}=\left\{\frac{-3+x^2(n+2)\mp\sqrt{2(3+(n+2)(x^2-2)\,x^2)}}{3+(n+2)(nx^2-2)\,x^2}\right\}^{-1/d}, \tag{30}$$

thus a minimum will occur for $l>l_{\min}$ and $l<l_{\max}$. Since the second solution ($l<l_{\max}$) is in the range $l\ll l_{\text{crit}}$, see Fig. 6, where the validity of the treatment does not hold anymore, this solution should be regarded as unphysical and is hence discarded leaving $l\gg l_{\min}$ only.

The third characteristic length (l_{sing} included in Fig. 6 results from the pole of the quantity $h_{\min}$ {(26)}, which is given by $(a_2-a_1)(b_2-b_1)=0$. As a detailed discussion of the quantity $h_{\min}$ shows {see [45]}, in cases of interest we also have $l_{\text{sing}}\ll l_{\text{crit}}$ and then this singularity is of no interest. Only for small x, namely for

$$x<x_+\equiv\sqrt{1+\sqrt{(n-1)/(n+2)}},$$

$l_{\min}$ and $l_{\max}$ do not exist {(30) would yield an imaginary solution then} and in this case it is only the range $l>l_{\text{sing}}$ that would allow physically meaningful solutions where minima of the cumulant exist. In this case for a value of l corresponding to $h_{\min}=(q+1)^{-1}$ the position of the minimum corresponds to T_c while for $l\to l_{\text{sing}}$ we would have $h_{\min}\to 0$ and consequently $T_{\min}\to-\infty$, which also implies that the vicinity of this singularity is not of physical interest.

But one can express in general terms the value $g(T_{\min})$ at the minimum of the cumulant in terms of the coefficients a_1, a_2, b_1, b_2 as

$$g(T_{\min})=\frac{n}{2}\left\{1+\frac{2}{n}-\frac{(a_2-a_1)^2}{4(b_2-b_1)(a_2\,b_1-a_1\,b_2)}\right\}. \tag{31}$$

From (26)–(31) it is easy to obtain the asymptotic behavior valid in the limit $l\to\infty$, namely

$$T_{\min}-T_c\xrightarrow{l\to\infty}(2A)^{-1}\ln(nx^2l^{-d}/q)\,l^{-d}, \tag{32}$$

$$g(T_{\min})\xrightarrow{l\to\infty}-l^d/(8x^2). \tag{33}$$

Thus the position of the minimum for large l differs from T_c only by a contribution inversely proportional to the system volume, apart from a logarithmic correction, while the depth of the minimum diverges towards minus infinity. Since the constant A is always negative, and the logarithm for large l as well, we have $T_{\min}>T_c$ generally. Since the order parameter dimensionality n has only a weak effect on $P_l(\phi)$ for large l {Fig. 9}, it is no surprise that n enters only in (32) via a logarithmic correction.

For the discussion of the intersections of the cumulants we calculate the crossing temperature T_{cross} for two neighboring system lengths l and $l'=l+\delta l$. Since we are mainly interested in the behavior for large volumes, we approximate $\exp\{-A(T-T_c)\,l^{-d}\}$ by 1, which is consistent with the numerical results and with an approximation for the intersections from tangents to the cumulants at T_c [45]. The expansion of the resulting T_{cross} and $g(T_{\text{cross}})$ in a power series in l^{-d} yields, for the ratio of susceptibilities $x^2=\chi_+/\chi_-+2q/n$,

$$T_{\text{cross}}-T_c\approx-A^{-1}\frac{1+q}{q}(2q-nx^2)\,l^{-2d}, \tag{34}$$

$$g(T=T_{\text{cross}})\approx1-\frac{n}{2q}+\frac{2n}{q^2}(1+q)(nx^2-2q)\,l^{-d}. \tag{35}$$

In particular the cumulant intersection occurs below T_c for $x^2=\chi_+/\chi_->2q/n$ and above T_c for $\chi_+/\chi_-<2q/n$. In the case $\chi_+/\chi_-=2q/n$, however, the crossing points for increasing systems lengths approach the transition point even faster, namely

$$T_{\text{cross}}-T_c\approx-A^{-1}\frac{2(1+q)}{n}(2nq+4q-3n)\,l^{-3d}, \tag{36}$$

$$g(T_{\text{cross}})\approx1-\frac{n}{2q}+3n\frac{1+q}{q}\left(3-2q-\frac{4q}{n}\right)l^{-2d}. \tag{37}$$

According to (34) and (36) the intersections of the cumulants differ from T_c only by terms of order $l^{-2d}\propto V^{-2}$ and V^{-3}, respectively, while the region over which finite size rounding is pronounced always is of order V^{-1}. For practical purposes, this small temperature region where the crossing occurs is indistinguishable from a unique intersection point at a universal cumulant value $g(T_{\text{cross}})\approx1-n/(2q)$.

3. First-order transitions with one-component order parameter ($n=1$)

Thise case is of practical interest (e.g. systems near a tricritical point, such as metamagnets or the Blume-Emery-Griffiths model [43] fall in this class), and it allows a rather explicit treatment. Thus we give some details on this case below.

Equation (24) can now be written more explicitly as

$$g_l(T)=\frac{1}{2}\left\{3-\frac{3hx^4\,l^{-2d}+(1-h)(1+6l^{-d}+3l^{-2d})}{[hx^2l^{-d}+(1-h)(1+l^{-d})]^2}\right\} \tag{38}$$

which has a minimum at (see (26), (27) for $n=1$)

$$h_{\min}=\frac{1+l^{-d}(7-2x^2)+3l^{-2d}(3-4x^2+x^4)+3l^{-3d}(x^2-1)^2}{1+l^{-d}(7-x^2)+3l^{-2d}(3-2x^2-x^4)+3l^{-3d}(1-x^2-x^4+x^6)}. \tag{39}$$

Using (28), (30), (39) {see also Fig. 6}, we find that for $x=1$ a minimum exists for arbitrary l, while a nontrivial condition results for $x>1$, a minimum exists for

$$l>l_{\min}=\{(3-\sqrt{6})/[3(x^2-1)]\}^{-1/d}, \tag{40}$$

(see (30) for $n=1$).

Figure 10a is an illustration which shows that indeed the minimum of $g_l(T)$ is seen only for $l>l_{\min}$, with $l_{\min}\approx 2.5$ in this case. Unfortunately, Fig. 6 shows that also $l_{\min}$ is comparable to l_{crit}, the linear dimension where the present approximations get inaccurate, and hence the minimum linear dimension $l_{\min}$ which must be reached in order that $g_l(T)$ exhibits a minimum cannot be reliably predicted. In the regime where the present approximations are accurate, i.e. for $l\gg l_{\text{crit}}$, we always have $l\gg l_{\min}$, and hence $g_l(T)$ exhibits a pronounced and deep minimum there. The value of this minimum {(31)} can be written explicitly

$$g(T_{\min})=-\frac{\{1+6(1-x^2)\,l^{-d}+3(1-x^2)^2\,l^{-2d}\}^2}{8x^2\,l^{-d}\{1+l^{-d}(7-4x^2)+ +3l^{-2d}(3-4x^2+x^4)+3l^{-3d}(x^2-1)^2\}}. \tag{41}$$

Figure 11 illustrates then the behavior of the cumulants near the intersection points. As expected from the analysis of the previous section, the fine resolution of both abscissa and ordinate of these plots shows that there is no unique intersection point, and the actual intersections can occur both for $T>T_c$ and for $T<T_c$, depending whether

$$x^2>2q/n=4 \quad \text{or} \quad x^2<4.$$

Comparing the actual intersections with the predictions of (34)–(37), quoted in the figure caption, show that there is reasonable agreement between the numerical results and these approximate formulae.

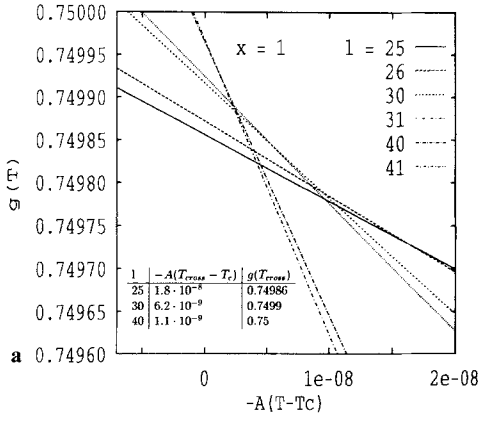

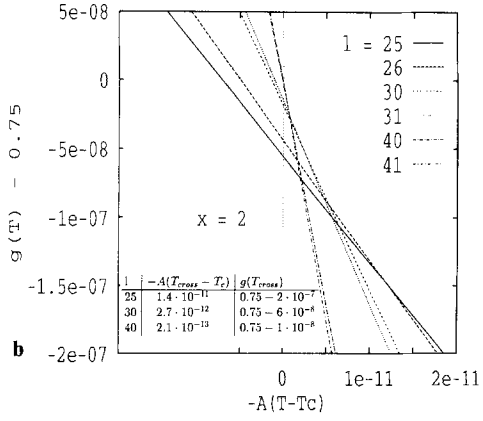

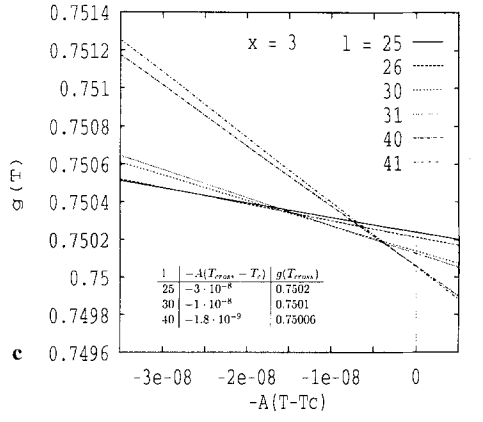

Fig. 11a–c. Cumulant $g(T)$ plotted vs. $-A(T-T_c)$ for $x=1$ **a**, $x=2$ **b** and $x=3$ **c**, showing three pairs of neighboring values of l, $l'=l+1$ in each case. The predictions of the approximations (34)–(37) are quoted in the inset

4. First-order transitions with two-component order parameter ($n=2$)

The present case is of interest for the $q=3$ state Potts model in $d=3$ dimensions, which is one of the standard models used for the study of weak first-order transitions by Monte Carlo simulation [48, 49]. Hence it may be useful to give some details on this case, too. The quantity $h_{\min}^{-1}-1$, which controls the shift of the minimum of the cumulant, (28), is given by

$$h_{\min}^{-1}-1 =\frac{2x^2l^{-d}+4x^2l^{-2d}(3-4x^2)+2x^2l^{-3d}[3+8x^2(x^2-1)]}{1+l^{-d}(7-4x^2)+l^{-2d}(9-24x^2+8x^4)+ +l^{-3d}(3-12x^2+8x^4)}. \tag{42}$$

The value of the cumulant at the minimum is

$$g(T_{\min})=2-\frac{(1+6l^{-d}+3l^{-2d}-8x^4l^{-2d})^2}{8l^{-d}x^2(1+l^{-d}-2l^{-d}x^2)\times \times(1+6l^{-d}+3l^{-2d}-4x^2l^{-d}-4x^2l^{-2d})}. \tag{43}$$

One should remember that this minimum for $x\geqq x_+=\sqrt{3/2}\approx 1.22$ occurs only if $l>l_{\min}$, cf. (30). Figure 12 gives an example where the predictions resulting from (42), (43) are compared to the straightforward numerical calculation of $g_L(T)$ using directly (23), (24). As it should be, the minima of $g_L(T)$ are consistent with (42), (43).

This figure also nicely illustrates the asymptotic behavior noted in (33), namely that $g(T_{\min})\to-\infty$ as $l\to\infty$.

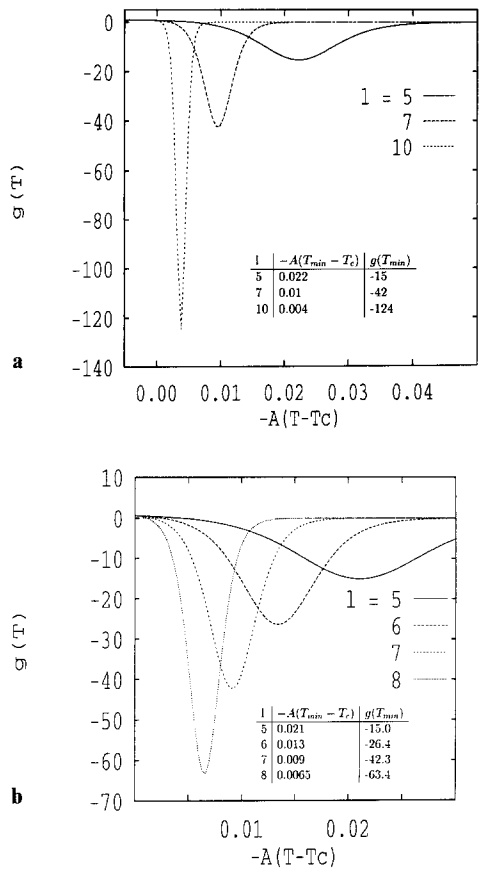

Fig. 12a, b. Plot of the reduced fourth-order cumulant $g_L(T)$ vs. the temperature variable t for the case $x=1$, $n=2$ and four values of l as indicated in the figure. Predictions for t at the minimum and $g(T_{\min})$ resulting from (28), (42), (43) are quoted in the inset

Again one can use the direct calculation of $g_L(T)$ to study cumulant intersections for pairs of neighboring values of large l – the general pattern of behavior is very similar to that of Fig. 11, apart from the fact that now all intersections occur close to $g(T_{\text{cross}}) \approx 2/3$ rather than $g(T_{\text{cross}}) \approx 3/4$ as for $n=1$ [45].

However, it should be noted that the approach to the asymptotic behavior not always is as fast as Figs. 10b and 12 suggest. While the convergence is fairly rapid for $x \lesssim 2$, a rather slow convergence is observed for larger x. E.g., for $x=3$ $g_L(T)$ for $3 \leqq l \leqq 5$ has an intersection in the region near $g \approx 0.75$, and for $x=4$ the intersection in this range of sizes even occurs near $g \approx 0.8$. Only for distinctly larger l can one then observe a convergence of the intersection ordinate to the asymptotic value, $g(T_{\text{cross}}) \approx 2/3$ [45, 39].

5. Discussion

The traditional treatment of finite size effects in the context of Monte Carlo studies of phase transitions [5, 6, 11, 13–15] discusses the order parameter distribution $P_L(m)$ and its moments for second-order transitions, while for thermally driven first-order transitions it is the distribution of internal energy $P_L(E)$ that is considered [25–36]. Obviously, this is unsatisfactory near multicritical points, where the order of the transition may change upon variation of parameters in the Hamiltonian, as well as for models where the order of the transition is controversial. It is natural to consider both distributions $P_L(m)$, $P_L(E)$ in all cases, of course, to make full use of the information contained in the Monte Carlo data. While the extension of finite size scaling at critical points to $P_L(E)$ is straightforward [50] and the finite-size rounding of the specific heat at critical points has been considered for a long time [9, 16, 51] the present paper is the first one that gives a detailed study of $P_L(m)$ at thermally driven first-order transitions. For the case of a n-component ordering with q distinct ordered phases (such as Potts ferromagnets where $n=q-1$), a phenomenological description similar in spirit to earlier discussions of $P_L(m)$ at field-driven transitions [22] was presented. We showed that the order parameter cumulant $g_L(T)$ for large L has a non-monotonic behavior, with a minimum $g(T_{\min}) \propto -L^d$ at a temperature $T_{\min}$ that differs from the first-order transition temperature T_c by an amount of order L^{-d}. This minimum occurs only if L exceeds a minimum size $L_{\min}$; however, $L_{\min}$ itself can no longer be reliably predicted from our treatment, since the assumptions made {each phase being described by a simple gaussian peak, interfacial contributions to $P_L(m)$ being neglected} then no longer are valid.

Thus the occurrence of the minimum of $g_L(T)$ at negative values of $g_L(T)$, with a tendency to become deeper and narrower as L increases, can be used as a qualitative indicator that a first-order transition occurs. For a quantitative analysis of such transitions, of course, it certainly is necessary to establish that the asymptotic regime of finite size scaling is reached (by verifying the predicted L-dependence of $T_{\min}$ and $g(T_{\min})$, for instance), and from estimations of the coefficients in various power laws found above the characteristics of the transitions {jump of the order parameter $M_{\text{sp}}(T_c)$ at the transition, susceptibility ratio χ_+/χ_-, etc.} can be extracted. Such an analysis of very accurate simulation work still remains to be done!

A particularly interesting feature is the occurrence of a sharp intersection point of the cumulants at a temperature T_{cross} and a value of

$$g(T_{\text{cross}})_{L\to\infty} = 1 - \frac{n}{2q}.$$

It has been shown that for typical cases this crossing points occur at a temperature T_{cross} that differs from T_c only by terms of order L^{-2d} (or L^{-3d}, for a special ratio χ_+/χ_-) and that $g(T_{\text{cross}})_L$ differs from $g(T_{\text{cross}})_{L\to\infty}$ only by terms of order L^{-d}. In the finite size scaling limit, where g_L is a function of order unity and $T-T_c$ is scaled with L^d, there is hence a simple universal behavior! This fact also implies that the cumulant intersection method qualifies as a good method to locate first-order transitions (just as it is a good method to locate second-order transitions, as is well known [1, 2, 5, 6, 11, 13–15, 17]). The mere fact of a "unique" cumulant intersection

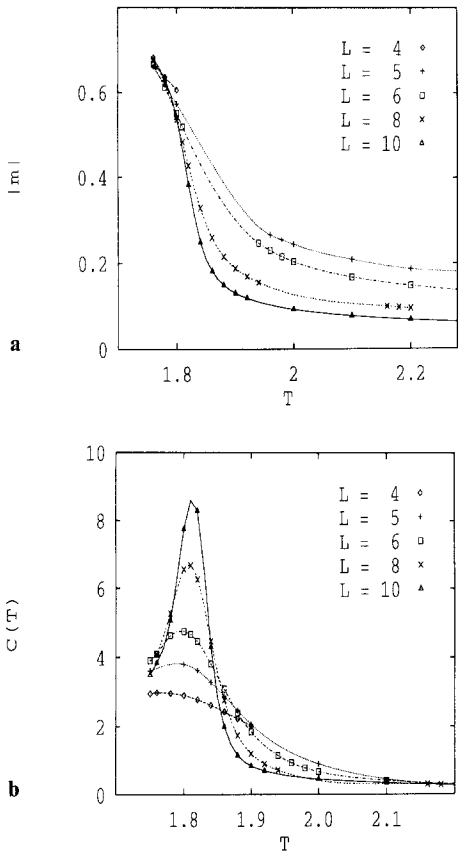

Fig. 13 a, b. Absolute value of the order parameter **a** and the specific heat **b** plotted vs. temperature T, for the three states Potts feromagnet in $d=3$ and several choices of L as indicated

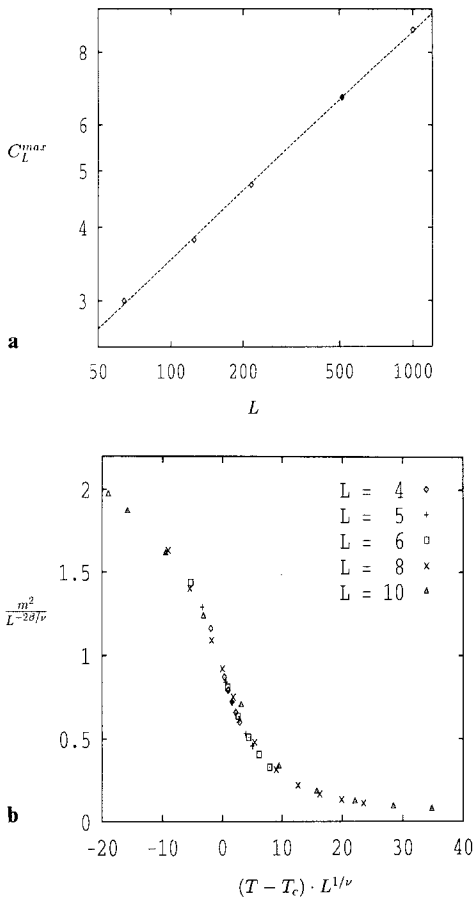

Fig. 14 a Log-log plot of the specific heat maximum $C_{\max}(L)$ vs. L, for the nearest-neighbor 3-state Potts ferromagnet. **b** Scaling plot for the mean magnetization square $m^2(T, L)$, choosing effective exponents $\nu_{\text{eff}}=0.4$, $\beta_{\text{eff}}=0.12$ and $T_c=1.8$

point should not, on the other hand, be taken as an evidence for a second-order transition! On the contrary, if the curves $g_L(T)$ cross for different L at a value close to $1-n/(2q)$, which value is known in beforehand if the nature of the ordering is understood, one rather has an indication of a first-order transition, while an intersection at one of the (known) universal values $g^*=g_L(T_c)$ for the various universality classes of second-order transitions can be taken as an evidence for the fact that the considered model has a critical point belonging to that universality class.

How well do these predictions work out in practice? Here we present a first preliminary test for the case of the $d=3$, $q=3$ nearest-neighbor Potts model only. With full intention, the bulk of our data is restricted to small L, $L\leqq 10$: for many models of real practical interest (e.g. models containing quenched disorder such as the Potts glass [52] larger values of L indeed are unavailable due to equilibration problems). Figure 13 shows now raw data for order parameter and specific heat $C_L(T)$. The order parameter indeed looks as it would look for second-order transitions, while the specific heat qualitatively resembles more the finite size behavior of first-order transitions. However, plotting the maximum values $C_L(T_{\max})=C_{\max}(L)$ versus L on a double logarithmic plot versus L (Fig. 14a), one does not find yet the exponent for a first-order transition $\{C_{\max}(L)\propto L^d=L^3\}$, but rather $C_{\max}(L)\propto L^{y_{\text{eff}}}$ with $y_{\text{eff}}=1.2$ {for a second order transition, we would expect $C_{\max}(L)\propto L^{\alpha/\nu}=L^{(2/\nu)-d}$, of course}. Also the data for the magnetization and its moments could be scaled just as for second-order transitions, e.g. $m^2(T, L)=L^{-2\beta/\nu}\tilde{f}\{L^{1/\nu}(T-T_c)\}$, with effective exponents $\beta_{\text{eff}}\approx 0.12$, $y_{\text{eff}}\approx 0.4$, $T_c\approx 1.81$, see Fig. 14b. This traditional "data collapsing" method [1] hence also would easily fail to correctly identify the order of the transition. Fig. 15 shows that the cumulants of both energy $\{V_L=1-\langle E^4\rangle/(3\langle E^2\rangle^2)\}$ and order parameter do point towards the possible existence of a first-order transition. However, while the energy cumulant (Fig. 15a) is far from the asymptotic regime – the minimum of the energy cumulant $V_{\min}(L)=V_L(T_{\min})$ has not at all converged to a limiting value yet! – the cumulant intersections for the order parameter (Fig. 15b, c) are rather close to the limiting value, $g(T_{\text{cross}})_{L\to\infty}=2/3$ in this case. Also the characteristic minimum of $g_L(T)$ is clearly seen – note the striking qualitative similarity of Fig. 15b and Fig. 10!

Thus we find that for the order parameter distribution and its cumulant much smaller sizes suffice to identify the order of the transition {and estimate the jump $m_{\text{sp}}(T_c)$} than for the energy distribution. This simply may be due to the fact that the order parameter jump

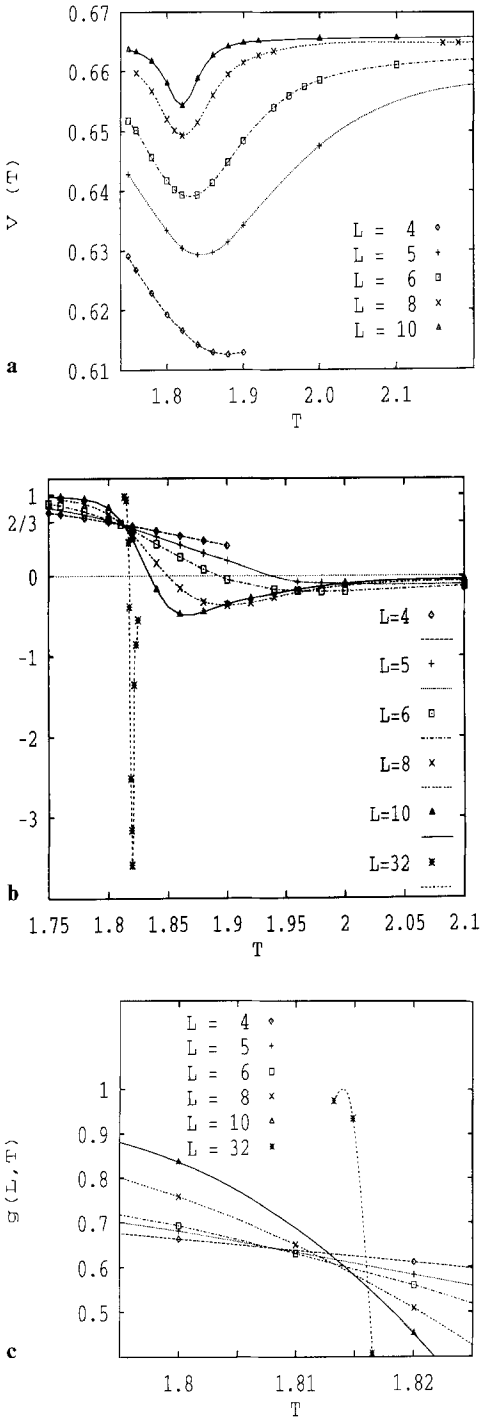

Fig. 15 a Energy cumulant $V_L(T)$ plotted vs. temperature for the three state Potts model in $d=3$. Several choices of L are shown as indicated in the figure. **b** Order parameter cumulant $g_L(T)$ plotted vs. temperature. **c** Detail from **b** near the "unique" intersection point of the cumulants in that figure. The "exact" value of $T_c = 1.8165$ is taken from [29] and [53]. Data for $L=32$ in **b** are due to M. Kikuchi (cf. also [37])

is large, $m_{sp}(T_c) \approx 0.46$ according to [53], while the jump in internal energy is relatively small $\{E_+ - E_- \approx 0.11$ [53]$\}$. It would be very interesting to check this behavior for the $d=2$ Potts model with $q>4$ states also, since a lot of exact information on the transition in that case is available [42] including the correlation length [54]. Of course, a closer comparison between Figs. 15b and 10 also reveals some minor differences. This must be expected, of course, since corrections of order $\exp(-L/\xi_+)$, $\exp(-L/\xi_-)$ where $\xi_+(\xi_-)$ are the correlation lengths of the disordered (ordered) phase near the transition must be expected to occur in all moments of the order parameter distribution. Such corrections have been disregarded throughout – this is legitimate if $L \gg \xi_+$, $L \gg \xi_-$, but clearly this regime was not reached with the data of Figs. 13–15. But the point of these data is that the analysis along the lines of the present theory allows a better diagnosis of the order of the transition even if $L \approx \xi_+$, ξ_- than the traditional approaches, although the present theory then is not quantitatively applicable.

This reserch was supported by the DFG under grant No. SFB262/D1. We acknowledge the grant of computer time at the CRAY-YMP of the HLRZ Jülich, and are grateful to Dr. M. Kikuchi for allowing us to include his data in Fig. 15b. We thank Dr. M. Tsypin for drawing our attention to [46].

References

1. Binder, K. (ed.): Monte Carlo methods in statistical physics. Berlin, Heidelberg, New York: Springer 1979
2. Binder, K. (ed.): Applications of the Monte Carlo method in statistical physics. Berlin, Heidelberg, New York: Springer 1984
3. Heermann, D.W.: Computer simulation methods in theoretical physics. Berlin, Heidelberg, New York: Springer 1986
4. Hoover, W.G.: Molecular dynamics. Heidelberg, Berlin, New York: Springer 1986
5. Binder, K., Heermann, D.W.: Monte Carlo simulation in statistical physics: an introduction. Berlin, Heidelberg, New York: Springer 1988
6. Binder, K. (ed.): The Monte Carlo method in condensed matter physics. Berlin, Heidelberg, New York: Springer 1992
7. Stanley, H.E.: An introduction to phase transitions and critical phenomena. Oxford: Oxford University Press 1971
8. Binder, K.: Rep. Progr. Phys. **50**, 783 (1987)
9. Fisher, M.E.: In: Green, M.S. (ed.) Critical phenomena, Proc. 1970 Enrico Fermi International School on Physics, p. 1. New York: Academic Press 1971
10. Barber, M.N.: In: Domb, C., Lebowitz, J.L. (eds.) Phase transitions and critical phenomena, Vol. 8, p. 145. New York: Academic Press 1983
11. Binder, K.: Ferroelectrics **73**, 43 (1987)
12. Cardy, J.L. (ed.): Finite size scaling. Amsterdam: North-Holland 1988
13. Privman, V. (ed.): Finite size scaling and numerical simulation of statistical systems. Singapore: World Scientific 1990
14. Binder, K.: Ann. Rev. Phys. Chem. **43**, 33 (1992)
15. Binder, K.: In: Lang, C..B., Gausterer, A. (eds.) Computational methods in field theory, p. 57. Berlin, Heidelberg, New York: Springer 1992
16. Binder, K., Rauch, H.: Z. Phys. **219**, 201 (1969); Binder, K.: Z. Angew. Phys. **30**, 51 (1970); Binder, K.: Physica **62**, 508 (1972)
17. Binder, K.: Z. Phys. B**43**, 119 (1981); Phys. Rev. Lett. **47**, 693 (1981)
18. Imry, Y.: Phys. Rev. B**21**, 2042 (1980)
19. Fisher, M.E., Berker, A.N.: Phys. Rev. B**26**, 2507 (1982)
20. Blöte, H.W.J., Nightingale, M.P.: Physics A**112**, 405 (1982); Cardy, J.L., Nightingale, M.P.: Phys. Rev. B**27**, 4256 (1983)
21. Privman, V., Fisher, M.E.: J. Stat. Phys. **33**, 385 (1983)
22. Binder, K., Landau, D.P.: Phys. Rev. B**30**, 1477 (1984)
23. Fisher, M.E., Privman, V.: Phys. Rev. B**32**, 447 (1985)
24. Privman, V., Rudnick, J.E.: J. Stat. Phys. **60**, 551 (1990)

25. Challa, M.S.S., Landau, D.P., Binder, K.: Phys. Rev. B**34**, 1841 (1986)
26. Borgs, C., Kotecky, R.: J. Stat. Phys. **61**, 79 (1990)
27. Borgs, C., Kotecky, R., Miracle-Sole, S.: J. Stat. Phys. **62**, 529 (1991)
28. Gavai, R.V., Karsch, F., Petersson, B.: Nucl. Phys. B**322**, 738 (1989)
29. Fukugita, M., Okawa, M.: Phys. Rev. Lett. **63**, 13 (1989)
30. Fukugita, M., Mino, H., Okawa, M., Ukawa, A.: J. Phys. A**23**, L561 (1990)
31. Billoire, A., Gupta, S., Irback, A., Lacare, R., Morel, A., Petersson, B.: Phys. Rev. B**42**, 6743 (1990); Nucl. Phys. B**258**, 231 (1990)
32. Peczak, P., Landau, D.P.: Phys. Rev. B**39**, 11932 (1990)
33. Lee, J., Kosterlitz, J.M.: Phys. Rev. Lett. **65**, 137 (1990); Phys. Rev. B**43**, 3265 (1991)
34. Billoire, A., Lacare, R., Morel, A.: Nucl. Phys. B**370**, 773 (1992)
35. Berg, B.A., Neuhaus, T.: Phys. Lett. L**3267**, 249 (1991); Phys. Rev. Lett. **68**, 9 (1992)
36. Borgs, C., Janke, W.: Phys. Rev. Lett. **68**, 1738 (1992)
37. Kikuchi, M., Okabe, Y.: J. Phys. Soc. Jpn. **61**, 3503 (1992)
38. Fukugita, M., Miro, H., Okawa, M., Ukawa, A.: J. Stat. Phys. **59**, 1397 (1990)
39. Binder, K., Vollmayr, K., Deutsch, H.-P., Reger, J.D., Scheucher, M., Landau, D.P.: Int. J. Mod. Phys. C**3** 1025 (1992)
40. Landau, L.D., Lifshitz, E.M.: Statistical physics. London: Pergamon Press 1984
41. Potts, R.B.: Proc. Comb. Philos. Soc. **48**, 106 (1952)
42. Wu, F.Y.: Rev. Mod. Phys. **54**, 235 (1982)
43. Lawrie, I.D., Sarbach, S.: In: Domb, C., Lebowitz, J.L. (eds.) Phase transitions and critical phenomena. Vol. 9, p. 1. New York: Academic Press 1984
44. Morris, J.R., Gooding, R.J.: Phys. Rev. B**43**, 6057 (1991); J. Stat. Phys. **67**, 471 (1992), R.J. Gooding: Scri. Met. **25**, 105 (1991)
45. Vollmayr, K.: Diplomarbeit (Universität Mainz, 1992, unpublished)
46. Stephanov, M.A., Tsypin, M.M.: Nucl. Phys. B**366**, 420 (1991)
47. Fisher, M.E.: Rev. Mod. Phys. **46**, 597 (1974)
48. Herrmann, H.J.: Z. Phys. B**35**, 1736 (1979); Knak-Jensen, S.J., Mouritsen, O.G.: Phys. Rev. Lett. **43**, 1736 (1979)
49. Blöte, H.W., Swendsen, R.H.: Phys. Rev. Lett. **43**, 799 (1979)
50. Milchev, A., Binder, K., Heermann, D.W.: Z. Phys. B**63**, 521 (1986)
51. Ferrenberg, A.M., Landau, D.P.: Phys. Rev. B**44**, 5881 (1991)
52. Scheucher, M., Reger, J.D., Binder, K., Young, A.P.: Phys. Rev. B**42**, 6881 (1990)
53. Wilson, W.G., Vause, C.A.: Phys. Rev. B**36**, 587 (1987)
54. Klümper, A., Schadschneider, A., Zittartz, J.: Z. Phys. B **76**, 247 (1989)